Kinetic and Mechanistic Studies on the Reaction of Dioxygen with Hexa-aquamolybdenum(III) †

Elaine F. Hills, Paul R. Norman, T. Ramasami, David T. Richens, and A. Geoffrey Sykes *
Department of Inorganic Chemistry, The University, Newcastle upon Tyne NE1 7RU

The reaction of hexa-aquamolybdenum(III) with O_2 in *p*-toluenesulphonic acid (Hpts) solutions, I = 2.0 M [Li(pts)], gives the di-μ-oxo-molybdenum(V) ion $[Mo_2O_4(H_2O)_6]^{2+}$ as product: $2Mo^{3+} + O_2 + 2H_2O \longrightarrow Mo_2O_4^{2+} + 4H^+$. Use of isotopically labelled O_2 followed by i.r. spectroscopy on the isolated $Mo_2O_4^{2+}$ has demonstrated that at least some ^{18}O is taken up in the μ-oxo-positions. With Mo^{3+} in large excess an intense yellow intermediate MoO_2Mo^{6+} (or a related form) with a peak at 395 nm (ε = 2 300 M^{-1} cm^{-1}) is observed. At 25 °C stopped-flow studies on the decay of this intermediate give rate constants $k_{3(obs.)}$ which can be expressed as in equation (i). The various constants are as defined in equations (ii)—(iv), where values indicated are for 2.0 M Hpts.

$$k_{3(obs.)} = \frac{K_1K_2k_3[Mo^{3+}]^2}{1 + K_1[Mo^{3+}] + K_1K_2[Mo^{3+}]^2} \qquad \text{(i)}$$

$$Mo^{3+} + O_2 \rightleftharpoons MoO_2^{3+} \qquad (K_1\ 360\ M^{-1}) \qquad \text{(ii)}$$

$$MoO_2^{3+} + Mo^{3+} \rightleftharpoons MoO_2Mo^{6+} \qquad (K_2\ 535\ M^{-1}) \qquad \text{(iii)}$$

$$MoO_2Mo^{6+} + 2H_2O \longrightarrow Mo_2O_4^{2+} + 4H^+ \qquad (k_3\ 0.23\ s^{-1}) \qquad \text{(iv)}$$

Estimates of rate constants for reactions (ii) and (iii) were obtained from studies on the formation of MoO_2Mo^{6+}. All parameters were further refined by an iterative fitting procedure using the program KINSIM for multi-step reactions. The values of k_1 (180 M^{-1} s^{-1}) and k_2 (42 M^{-1} s^{-1}) are in excess of previous substitution rate constants for Mo^{3+}. With O_2 in excess of Mo^{3+} (0.72×10^{-4} M) there was no evidence for MoO_2Mo^{6+}, and an alternative route for conversion of MoO_2^{3+} to $Mo_2O_4^{2+}$, which is first order in MoO_2^{3+} (k_4 = 0.037 s^{-1}) was identified. In the refinement this step was included alongside (ii)—(iv). The reactions of MoO_2Mo^{6+} (k_3) and MoO_2^{3+} (k_4) exhibit $[H^+]^{-1}$ dependences consistent with an increase in hydrolysis of the metal ion.

Reactions of dioxygen with transition-metal ions in solution continue to attract much attention because of their fundamental importance and relevance to chemical and biological processes.[1] Although outer-sphere oxidations have been identified,[2] in many cases the products are consistent with inner-sphere processes.[3] Extensive studies on the reactions of cobalt(II) complexes with O_2 have led to the identification of 1:1 adducts formulated as Co^{III}–O_2^-, as well as 2:1 μ-peroxo-cobalt(III) products of the kind CoO_2Co^{4+}.[3,4] Other studies on the reaction of O_2 with single-electron reductants such as Cr^{II},[5] Ru^{II},[2a,6] Fe^{II},[7] and Cu^{I} [8] have been carried out. In contrast, very little is known about reactions in which the metal undergoes a two-electron change.[9] The reaction of hexa-aquamolybdenum(III) with O_2 provides an example of this kind. Earlier work has demonstrated that the molybdenum(V) aqua-dimer $Mo_2O_4^{2+}$ is the final product,[10] and that further oxidation to Mo^{VI} is slow.[11,12] The reaction raises questions as to whether intermediates having co-ordinated O_2^- and/or O_2^{2-} are formed, and whether Mo^{IV} is implicated as an intermediate. The only stable aqua-ion of Mo^{IV} is the trimer $Mo_3O_4^{4+}$,[13] a form which is not always readily accessible.[14] Monomeric and dimeric aquamolybdenum(IV) ions have yet to be identified and may only exist as transients. Any additional information concerning the substitution properties of $[Mo(H_2O)_6]^{3+}$ is also of interest.[11,15] The studies described are in aqueous acidic media, pH < 1, under which condition we choose to refer to the aquamolybdenum(III) ion as Mo^{3+}.

Experimental

Materials.—Hexa-aquamolybdenum(III) was obtained by aquation of hexachloromolybdate(III), $K_3[MoCl_6]$ (Climax Molybdenum), under rigorous air-free conditions as already described.[10,16] Since Mo^{III} is known to react with perchlorate,[12] *p*-toluenesulphonic acid, Hpts (Sigma Chemicals), was used. The reaction mixture resulting from the aquation of $K_3[MoCl_6]$ was chromatographed on an ice-cooled Dowex 50W-X8 column to separate the hexa-aqua Mo^{3+} ion from $Mo_2O_4^{2+}$ and other impurities. The desired product (*ca.* 0.06 M) was eluted with Hpts (2.0 M) using Teflon needles and rigorous O_2-free conditions. Absorption peaks for Mo^{3+} at 310 nm (ε 23.2 M^{-1} cm^{-1}) and 380 nm (ε 14.1 M^{-1} cm^{-1}) were in agreement with earlier work.[17] The concentration of H^+ in solutions of Mo^{3+} was determined by exchanging the metal ion for H^+ on an ion-exchange column and titrating the total $[H^+]$ against standard NaOH.

The concentration of O_2 in an oxygen-saturated 2.0 M Hpts solution was obtained by the method of Stone and Eichelberger.[18] This involved addition of Cr^{2+}, and determination of the unreacted excess iodometrically by a procedure involving addition of iodate. At 25 °C the solubility of O_2 in 2.0 M Hpts is

---

† *Non-S.I. unit employed:* M = mol dm^{-3}.

$(1.05 \pm 0.05) \times 10^{-3}$ M, which compares with a value of 1.41×10^{-3} M in H_2O at 25 °C.[19]

Lithium *p*-toluenesulphonate was prepared by neutralisation of the acid with lithium carbonate (Koch-Light), followed by recrystallisation.

A solution of aqua $Mo_2O_4^{2+}$ in 2 M Hpts,[16] and crystalline samples of the barium salt of $[Mo_2O_4(C_2O_4)_2(H_2O)_2]^{2-}$ and the di-μ-sulphido-analogue $[Mo_2O_2S_2(C_2O_4)_2(H_2O)_2]^{2-}$, were prepared by procedures similar to those already described.[20,21] Cylinder O_2 gas and >90% ^{18}O-labelled O_2 (both from B.O.C. Ltd.) were used without further purification.

Products and Stoicheiometry.—These were established by analysis of u.v.–visible spectra. The $Mo_2O_4^{2+}$ ion has absorption peaks at 295 nm (ε = 3 550 M^{-1} cm^{-1}) and 384 nm (ε = 103 M^{-1} cm^{-1}), both ε values being per dimer.[12] With $[O_2] = (1.3$—$9.8) \times 10^{-4}$ M and $[Mo^{3+}] = (0.036$—$19.2) \times 10^{-3}$ M at $[H^+] = 2.00$ M, $Mo_2O_4^{2+}$ is the sole molybdenum product, and the $[Mo_2O_4^{2+}]/[O_2]$ ratio of 1.03 ± 0.05 (six determinations) is in accord with a reactant stoicheiometry of 2:1 as in equation (1). On bubbling O_2 gas through Mo^{3+} at higher

$$2Mo^{3+} + O_2 + 2H_2O \longrightarrow Mo_2O_4^{2+} + 4H^+ \quad (1)$$

concentrations (2.3×10^{-2} M) in 2.0 M Hpts, conditions not appropriate to the kinetic studies, *ca.* 10% of the molybdenum product was present as the molybdenum(IV) aqua-ion $Mo_3O_4^{4+}$ (peak at 505 nm, ε per Mo = 56 M^{-1} cm^{-1}).[22]

Spectrum of Intermediate.—Preliminary studies revealed that there was a build-up of an intermediate with an intense absorption band at 395 nm. For the conditions investigated it was found that formation of the intermediate was most extensive at high $[H^+]$ (2.0 M) and high $[Mo^{3+}]$ (1.9×10^{-2} M). The shape of the spectrum (Figure 1) was obtained by using $[O_2] = 5.3 \times 10^{-4}$ M and $[Mo^{3+}] = 1.2 \times 10^{-2}$ M both at $[H^+] = 2.0$ M on the stopped-flow at 25 °C, and varying the wavelength for each point. From the KINSIM fits described below a value for ε at 395 nm of 2 300 ± 50 M^{-1} cm^{-1} per dimer was determined.

Product Analysis using Isotopically Labelled Oxygen.—Evidence for the incorporation of oxygen in the $Mo_2O_4^{2+}$ product was sought by isotopic labelling in which $^{18}O_2$ was reacted with Mo^{3+}, and the $Mo_2O_4^{2+}$ product examined for ^{18}O incorporation. Two identical experiments were carried out in which solutions of $^{16}O_2$ and $^{18}O_2$ were reacted with Mo^{3+} using an $Mo^{3+}:O_2$ ratio of 5:1. The reaction product was loaded onto a deaerated Dowex 50W-X8 column (7 × 0.8 cm), and the $Mo_2O_4^{2+}$ separated from unreacted Mo^{3+} under rigorously air-free conditions. Solutions of $Mo_2O_4^{2+}$ obtained were diluted to 0.1 M acid and re-adsorbed onto a Dowex 50W-X2 column (7 × 1.0 cm). The column was washed with 0.1 M HCl and the $Mo_2O_4^{2+}$ eluted with 2 M HCl. If the concentration of $Mo_2O_4^{2+}$ from the first column was <0.1 M, the procedure was repeated a third time. To a solution of $Mo_2O_4^{2+}$, *ca.* 0.1 M in dimer and 2.0 M in $[H^+]$, sodium oxalate (0.5 g) was added and the pH adjusted to 1.5. The barium salt of the oxalatomolybdenum(V) complex was obtained by careful addition of solid $BaCl_2$. Barium oxalate impurity (if any) was removed by recrystallisation from aqueous NH_4Cl. The structure of the oxalato-complex $[Mo_2O_4(C_2O_4)_2(H_2O)_2]^{2-}$ has been established and is as illustrated.[19] The

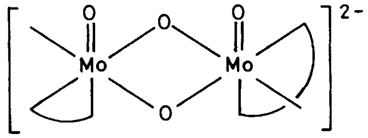

same procedure was used for the isolation of products from both the $^{18}O_2$ and $^{16}O_2$ reactions. The oxalato-complexes were characterised by i.r. spectroscopy in the 1 000—350 cm^{-1} region using KBr discs.

Unfortunately both μ-oxo- and oxalate ligands give bands in the 800—700 cm^{-1} region of interest. To help make assignments the barium salt of $[Mo_2O_2S_2(C_2O_4)_2(H_2O)_2]^{2-}$ was isolated by adopting the procedure described for the caesium salt.[21] It has been confirmed from crystallography[21] that the latter has two μ-sulphido- and no μ-oxo-ligands. From Figure 2 the band at 790 cm^{-1} for both the $Mo_2O_4^{2+}$ and $Mo_2O_2S_2^{2+}$ derivatives is attributed to oxalate ligand-centred vibrations. Comparison of the $^{16}O_2$ and $^{18}O_2$ products demonstrates that the ^{18}O label does at least partially occur in the bridging position. The occurrence of the oxalate band in the region of interest precludes any quantitative analyses of the spectrum. The need to observe kinetic conditions in which the amount of dissolved O_2 was low ($<5.2 \times 10^{-4}$ M) limited detailed investigation of complexes other than with oxalate. Nevertheless the reduction in the relative intensity of the band at 780 cm^{-1} and enhancement of the intensity at 735 cm^{-1} (Figure 2), with a shift to a peak at 720 cm^{-1} in the case of the $^{18}O_2$ product, is of interest. Any incorporation of the $^{18}O_2$ label in the terminal oxo-position would have escaped our detection because of the time delay involved in the precipitation of the oxalato-complex. Exchange of ^{18}O in the terminal oxo-position with solvent is known to occur within a few minutes at 4 °C.[23,24] The observation of the ^{18}O label in the bridging oxygen position supports other evidence that an intermediate containing co-ordinated O_2 is formed.

Kinetics.—The reaction of Mo^{3+} with O_2 was studied at 25 °C, $I = 2.05 \pm 0.05$ M [Li(pts)], $[H^+] = 1.00$—2.00 M, with $[Mo^{3+}] = (1.5$—$19.2) \times 10^{-3}$ M in 10-fold excess of $[O_2] = (1.5$—$5.3) \times 10^{-4}$ M. Kinetic effects attributed to pts^- complexing with Mo^{3+} (ref. 17) are not apparent in the fast stopped-flow $[IrCl_6]^{2-}$ oxidation of Mo^{3+},[17] and do not appear to be influential in the present study. It would appear that any pts^- complex present initially is not replenished sufficiently rapidly to affect the kinetics of the faster redox reactions. The formation of the intermediate, which required up to *ca.* 30 s depending on

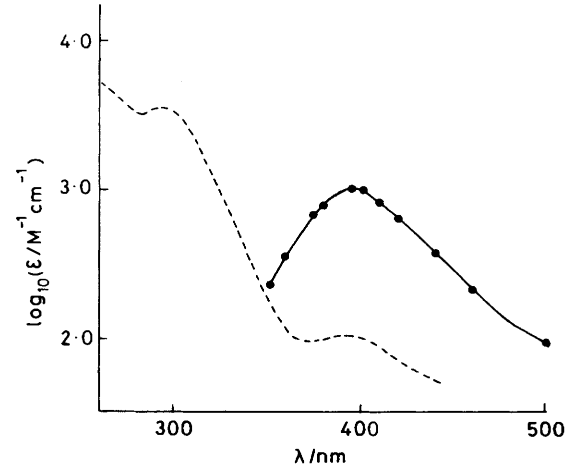

Figure 1. Spectra of the intermediate (——) and the aquamolybdenum(V) ion $Mo_2O_4^{2+}$ (- - -) formed in the reaction of Mo^{3+} (12.3×10^{-3} M) with O_2 (5.3×10^{-4} M) at 25 °C, in 2.0 M Hpts. The spectrum of the intermediate was determined (point by point) using stopped-flow mixing, and the ε at the peak position represents a lower limit

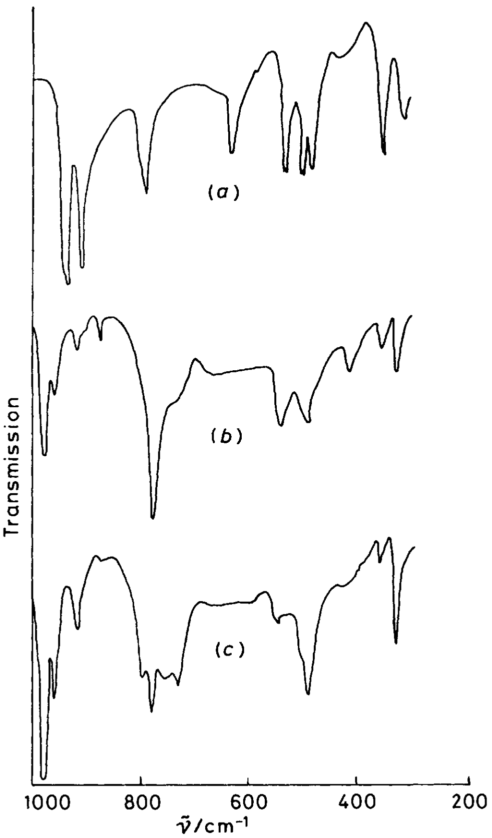

Figure 2. I.r. spectra of molybdenum(V) oxalato-complexes (*a*) $[MoO_2S_2(C_2O_4)_2(H_2O)_2]^{2-}$, (*b*) $[Mo_2O_4(C_2O_4)_2(H_2O)_2]^{2-}$, and (*c*) $[Mo_2O_4(C_2O_4)_2(H_2O)_2]^{2-}$ from an experiment using $^{18}O_2$. Bands in the 800—700 cm^{-1} range for (*a*) are diagnostic of oxalate, and in (*b*) and (*c*) for the μ-oxo-ligand. Additional bands in this same region for (*c*) provide evidence for incorporation of ^{18}O in the μ-oxo-positions

concentrations, was monitored at 395 nm, Figure 1. Decay of the intermediate was incident before complete formation could be observed. A standard consecutive reaction treatment[25] of the kind $A \longrightarrow B \longrightarrow C$ was used to obtain estimates of rate constants for processes leading to the formation of the intermediate.

At 295 nm and 25 °C absorbance changes for the conversion of the intermediate, formula MoO_2Mo^{6+} (or a closely related form), to $Mo_2O_4^{2+}$ are small, and independent monitoring of $Mo_2O_4^{2+}$ formation was not possible.

Some runs with O_2 in excess were also carried out.

Instruments.—Perkin-Elmer 554 and Lambda 5 u.v.–visible spectrophotometers and a Dionex D110 stopped-flow spectrophotometer were used. Infrared spectra were recorded on a Perkin-Elmer 598 spectrometer. The transfer of $^{18}O_2$ into small vessels was carried out on a vacuum line.

Treatment of Data.—Parameters were first obtained for graphical methods using a least-squares treatment. Further refinement was achieved by use of the KINSIM simulation program[26] obtained from Professor Frieden at the University of Washington, St. Louis, Missouri, and implemented on a VAX 11/780 computer. Manual iteration of the input parameters K_1, K_2, k_3, k_4, and ε for the intermediate at 395 nm were employed to fit a simulated reaction profile to the experimentally obtained data. The best fit was obtained by minimising the sum of the squares of the residual between simulated and experimental data. The spread of acceptable values was used to determine errors in the input parameters.

Table 1. Rate constants $k_{3(obs.)}$ and estimates of $k_{2(obs.)}$ for the third and second stages respectively of the reaction of Mo^{3+} with O_2, (1.5—5.3) × 10^{-4} M at 25 °C, I = 2.05 ± 0.05 M [Li(pts)], using a consecutive reaction treatment

$[H^+]$	$10^3[Mo^{3+}]$	$k_{3(obs.)}$	$k_{2(obs.)}$
M		s^{-1}	
2.00	19.2	0.205	0.89
2.0	14.6	0.199	0.68
1.1	14.6	0.330	0.68
2.0	10.6	0.184	0.56
1.5	10.6	0.243	0.58
1.0	10.6	0.270	0.62
2.0	7.1	0.169	0.39
2.0	7.0	0.158	0.49
1.5	7.0	0.182	0.40
1.0	7.0	0.261	0.44
2.0	6.1	0.154	0.35
2.0	6.0	0.158	0.35
2.0	3.9	0.127	0.26
2.0	2.9	0.104	0.21
1.0	2.9	0.139	0.27
0.75	2.9	0.182	0.31
2.0	2.0	0.070	0.173
1.5	2.0	0.088	0.187
1.0	2.0	0.084	0.187
2.0	1.5	0.053	0.157
2.0	1.2	0.031	
2.0	0.6	0.011	

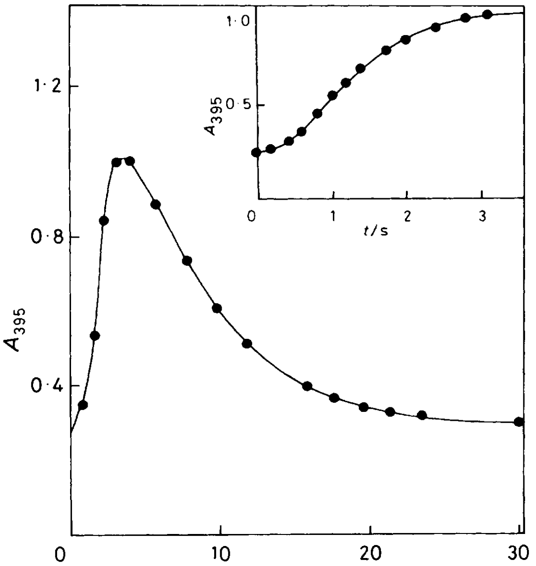

Figure 3. Identification of three stages in the reaction of Mo^{3+} (10.6 × 10^{-3} M) with O_2 (5.3 × 10^{-4} M) at 25 °C, in 2.0 M Hpts. Absorbance changes at 395 nm are shown (path length 1.67 cm). The inset illustrates the first two stages leading to the formation of the intermediate, and the main figure the formation and decay of the intermediate

Results

At 25 °C with Mo^{3+} in large excess three stages were observed using the stopped-flow method, Figure 3. Formation of an

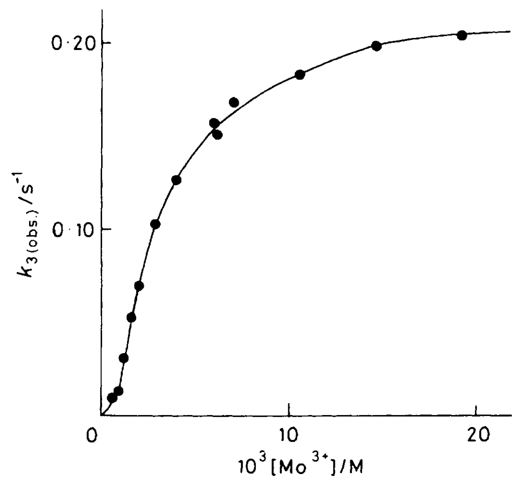

Figure 4. The reaction of O_2 with Mo^{3+} (reactant in excess) in 2.0 M Hpts. Variation of rate constants $k_{3(obs.)}$ (25 °C) for the decay of the intermediate with increasing $[Mo^{3+}]$

Table 2. Estimates of rate constants $k_{1(obs.)}$ and $k_{2(obs.)}$ at 25 °C for the first and second stages of the reaction of Mo^{3+} with O_2, (1.5—5.3) × 10^{-4} M, using a consecutive reaction treatment, $I = 2.05 \pm 0.05$ M [Li(pts)]

$[H^+]$	$10^3[Mo^{3+}]$	$k_{3(obs.)}$	$k_{2(obs.)}$
M		s^{-1}	
2.0	19.2	1.37	3.9
2.0	14.6	0.75	3.7
1.1	14.6	0.83	3.2
2.0	10.6	0.94	3.1
1.5	10.6	0.75	2.3
1.0	10.6	0.92	2.6
2.0	7.0	0.69	2.1
1.5	7.0	0.73	2.3
1.0	7.0	0.78	2.3
2.0	5.4	0.52	1.87
1.5	5.4	0.42	1.63
1.0	5.4	0.36	2.15
2.0	3.9	0.52	1.44
2.0	2.0	0.22	0.89
1.5	2.0	0.43	0.94
1.0	2.0	0.26	0.87

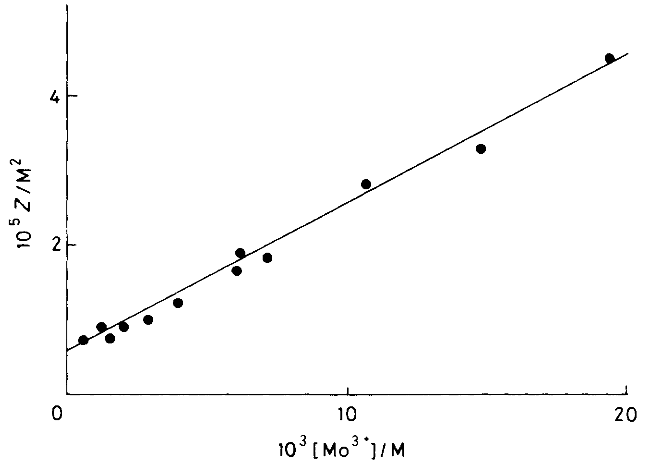

Figure 5. The dependence of Z, the left-hand side of equation (6), on $[Mo^{3+}]$ for the reaction of O_2 with Mo^{3+} (reactant in excess) at 25 °C in 2.0 M Hpts. Procedure for the determination of K_1 and K_2 using measured $k_{3(obs.)}$ and k_3 from Figure 4

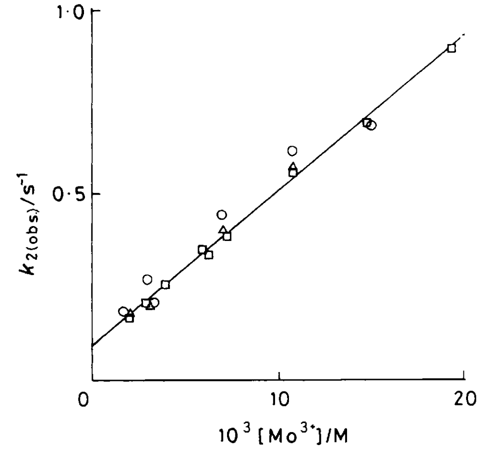

Figure 6. The dependence of $k_{2(obs.)}$ (25 °C) for the second stage of the reaction of O_2 with Mo^{3+} (reactant in excess) on $[Mo^{3+}]$ at $[H^+]$ = 2.0 (□), 1.5 (△), and 1.0 M (○), I = 2.0 M [Li(pts)]

intense yellow intermediate (Figure 1) is observed prior to formation of $Mo_2O_4^{2+}$. First-order kinetic plots for the decay of the intermediate at 395 nm gave $k_{3(obs.)}$, Table 1. No dependence on O_2 was observed. Once linearity is established such plots are linear to >90% completion of reaction. The variation of $k_{3(obs.)}$ with $[Mo^{3+}]$ in 2 M Hpts is illustrated in Figure 4. Consistent with three stages and the formation of an intermediate the mechanism in equations (2)—(4) is proposed. In this sequence k_3 is preceded by two relatively fast equilibria K_1 and K_2. Consideration of these three steps gives expression (5). At high $[Mo^{3+}]$, $k_{3(obs.)}$ approaches an upper limit of 0.23 ± 0.01 s^{-1} (Figure 4) equal to k_3. A number of tests of the rate equation (5) were carried out. On rearranging (5), equation (6) is obtained. A linear graph is obtained by plotting the left-hand side (Z) against $[Mo^{3+}]$, Figure 5. From the slope and intercept we obtain $K_1 = 395 \pm 15$ M^{-1} and $K_2 = 494 \pm 15$ M^{-1}. If the term in unity on the lower line of equation (5) is ignored then K_1 cancels, and a plot of $k_{3(obs.)}$ calculated using this modified equation and known parameters against $[Mo^{3+}]$, although lying close to the experimentally derived curve in Figure 4, gives no inflexion at low $[Mo^{3+}]$ close to the origin. It is clear that K_1 contributes most to the rate law at the smaller $[Mo^{3+}]$ values. In order to generate precisely the shape in Figure 4 a value of K_1 in the range 300—500 M^{-1} is required.

$$Mo^{3+} + O_2 \underset{k_{-1}}{\overset{k_1}{\rightleftharpoons}} MoO_2^{3+} \tag{2}$$

$$MoO_2^{3+} + Mo^{3+} \underset{k_{-2}}{\overset{k_2}{\rightleftharpoons}} MoO_2Mo^{6+} \tag{3}$$

$$MoO_2Mo^{6+} \xrightarrow{k_3} \text{product} \tag{4}$$

$$k_{3(obs.)} = \frac{K_1K_2k_3[Mo^{3+}]^2}{1 + K_1[Mo^{3+}] + K_1K_2[Mo^{3+}]^2} \tag{5}$$

$$\frac{k_3[Mo^{3+}]^2}{k_{3(obs.)}} - [Mo^{3+}]^2 = \frac{1}{K_1K_2} + \frac{1}{K_2}\cdot[Mo^{3+}] \tag{6}$$

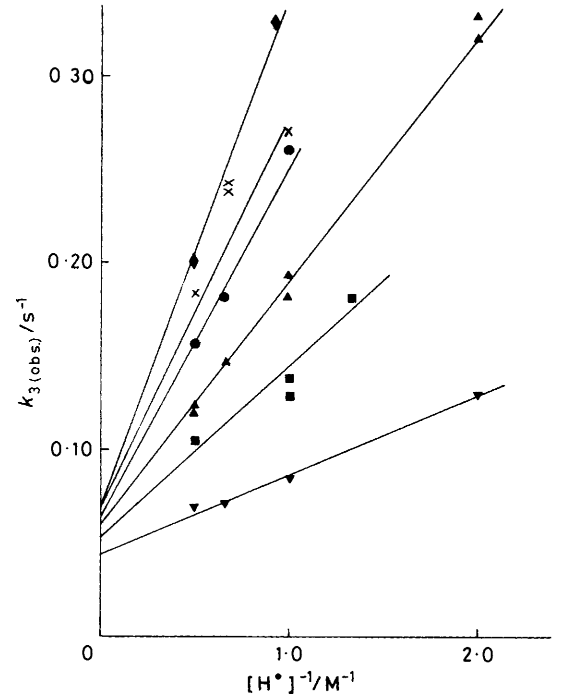

Figure 7. The dependence of $k_{3(obs.)}$ (25 °C) on $[H^+]^{-1}$ for the reaction of O_2 with Mo^{3+} (reactant in excess) with 10^3 $[Mo^{3+}]$ = 2.0 (▼), 2.9 (■), 5.4 (▲), 7.0 (●), 10.6 (×), and 14.7 M (◆), I = 2.0 M [Li(pts)]

Estimates of k_2 and k_{-2} were obtained by applying a consecutive treatment[25] for A ⟶ B ⟶ C to the second and third stages of reaction (Figure 3). This gave $k_{3(obs.)}$ (as already considered) and $k_{2(obs.)}$ respectively, Table 1. As can be seen from Figure 6, $k_{2(obs.)}$ exhibits a linear dependence on $[Mo^{3+}]$. The existence of an intercept (k_{-2}) suggests equilibration kinetics, equation (7). No dependence on $[H^+]$ is indicated,

$$k_{2(obs.)} = k_2[Mo^{3+}] + k_{-2} \qquad (7)$$

and from a least-squares fit of all $k_{2(obs.)}$ values k_2 = 40.5 ± 1.8 M^{-1} s^{-1} and k_{-}^{2} = 0.125 ± 0.015 s^{-1}. From the ratio of the two rate constants K_2 is 324 ± 60 M^{-1}, which is less than the value (494 M^{-1}) obtained from the more reliable approach using equation (6).

Estimates of k_1 and k_{-1} were obtained from a similar non-rigorous consecutive treatment of absorbance changes for the first two stages of reaction, Table 2. For this procedure, the maximum absorbance of the intermediate in each individual run was taken as A_{∞}. The values of $k_{2(obs.)}$ were more scattered (up to twice as big) compared to those in Table 1, and gave k_2 = 52.5 ± 7.2 M^{-1} s^{-1} and k_{-2} = 0.23 ± 0.075 s^{-1}. From their ratio K_2 is 228 ± 145 M^{-1}. There was also some scatter of $k_{1(obs.)}$, but again a first-order dependence on $[Mo^{3+}]$ and equilibration kinetics as in equation (7) were indicated. No dependence on $[H^+]$ was apparent and from a least-squares fit k_1 = 180 ± 14 M^{-1} s^{-1} and k_{-1} = 0.76 ± 0.13 s^{-1}, from which K_1 = 237 ± 70 M^{-1}.

Whereas for equilibria (2) and (3) no $[H^+]$ dependences are indicated for the $[H^+]$ range 1.0—2.0 M investigated, $k_{3(obs.)}$ exhibits an $[H^+]^{-1}$ dependence which at constant $[Mo^{3+}]$ can be expressed as in equation (8), Figure 7. Both a and b are dependent on $[Mo^{3+}]$ as in equation (5).

$$k_{3(obs.)} = a + b[H^+]^{-1} \qquad (8)$$

Table 3. First-order constants, $k_{4(obs.)}$, at 25 °C for the O_2 oxidation of Mo^{III} (O_2 in excess) obtained at λ = 295 nm, I = 2.05 ± 0.05 M [Li(pts)]

$[H^+]$	$10^4[O_2]$	$10^4[Mo^{3+}]$	$10^3k_{4(obs.)}$
M			s^{-1}
2.0	2.1	0.36	2.1
2.0	3.5	0.72	3.7
1.0	3.5	0.72	4.8
0.73	3.5	0.72	5.1
2.0	4.9	0.72	4.4
1.5	4.9	0.72	5.3
1.0	4.9	0.72	6.1
2.0	7.0	0.72	6.1
2.0	9.8	1.43	8.8
2.0	9.8	0.72	8.4
2.0	9.8	0.36	7.7

Table 4. Comparison of parameters obtained by (A) a graphic method and (B) a fit of data by KINSIM at 25 °C, I = 2.05 ± 0.05 M [Li(pts)]

Parameter	Method (A)	Method (B)
K_1/M^{-1}	395 ± 15*	420 ± 30
$k_1/M^{-1}\ s^{-1}$	180 ± 14	180 ± 7
k_{-1}/s^{-1}	0.76 ± 0.13	0.47 ± 0.02
K_2/M^{-1}	494 ± 15*	540 ± 30
$k_2/M^{-1}\ s^{-1}$	40.5 ± 1.8	42 ± 3
k_{-2}/s^{-1}	0.125 ± 0.115	0.08 ± 0.02
k_3/s^{-1}	0.23 ± 0.01*	0.23 ± 0.003
k_4/s^{-1}	0.021 ± 0.002	0.037 ± 0.005

* 2.0 M Hpts runs only.

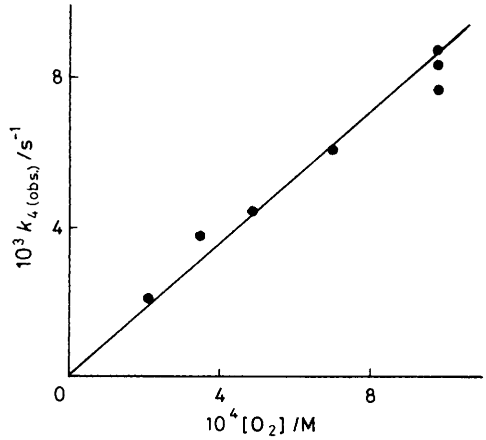

Figure 8. The dependence of rate constants $k_{4(obs.)}$ (25 °C) for the reaction of Mo^{3+} with O_2 (reactant in excess) on the concentration of O_2, I = 2.0 M [Li(pts)]

Finally, the reaction was studied with O_2 in large excess. Because of the relatively low solubility of O_2, small concentrations of Mo^{3+} had to be used. There was no evidence for any build-up of intermediate at 395 nm, which for the maximum $[Mo^{3+}]$ might have resulted in an absorbance as high as 0.3 if all the $[Mo^{3+}]$ had been converted to MoO_2Mo^{6+}. The formation of $Mo_2O_4{}^{2+}$ was monitored at 295 nm. A first-order dependence on $[O_2]$ was indicated, Figure 8, with little or no dependence of $k_{4(obs.)}$ on $[Mo^{3+}]$. A reaction sequence (9) and (10) is consistent with the rate law (11), from which it follows that $k_{4(obs.)} = k_4K_1[O_2]$. The slope in Figure 8 gives k_4K_1 =

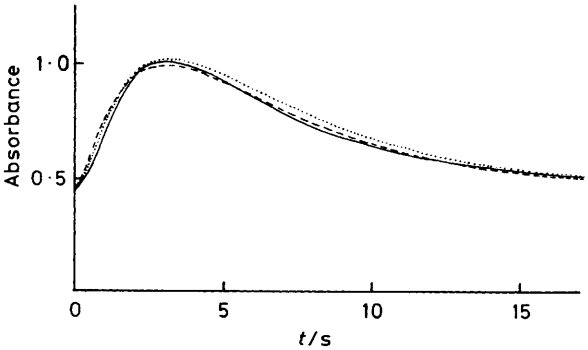

Figure 9. The variation of absorbance at 395 nm with time for the reaction of Mo^{3+} (14.6×10^{-3} M) with O_2 (2.62×10^{-4} M) at 25 °C in 2.0 M Hpts, $I = 2.0$ M. Experimental changes (——), simulated changes including k_4 (– – –), and simulated changes excluding k_4 (• • • •) are shown

8.4 ± 0.4 M^{-1} s^{-1} and hence, using K_1 from Table 4, $k_4 = 0.021 \pm 0.002$ s^{-1} in 2.0 M Hpts. From the $[H^+]$ variation (0.73—2.0 M), Table 3, k_4 exhibits a dependence on $[H^+]^{-1}$. This we fitted to an equation of the form (12). From data at $[Mo^{3+}] = 0.72 \times 10^{-4}$ M and $[O_2] = 3.5 \times 10^{-4}$ M, $c = 0.021 \pm 0.003$ s^{-1} and $d = 0.012 \pm 0.003$ M s^{-1}.

$$Mo^{3+} + O_2 \xrightleftharpoons{K_1} MoO_2^{3+} \quad (9)$$

$$MoO_2^{3+} \xrightarrow{k_4} \text{product} \quad (10)$$

$$d[Mo_2O_4^{2+}]/dt = k_4K_1[Mo^{3+}][O_2] \quad (11)$$

$$k_4 = c + d[H^+]^{-1} \quad (12)$$

The evaluation of k_3, K_1, and K_2 by graphical methods, and of approximate values of k_1, k_{-1}, and k_2, k_{-2} using a standard consecutive reaction treatment, was followed by the application of the KINSIM program[26] to obtain a refinement of all parameters. The program was applied to runs at 25 °C with $10^3[Mo^{3+}] = 14.6$, 10.6, 7.0, and 2.9 M and $10^4[O_2] = 2.62$, 5.25, 4.20, and 2.8 M respectively at $[H^+] = 2.0$ M, Figure 9. The fit of data at higher concentrations of Mo^{3+} was excellent, but at lower $[Mo^{3+}]$ the fit was less satisfactory due to the smaller (less than pseudo-first-order) excess of Mo^{3+}. A comparison of both sets of parameters is made in Table 4, where the KINSIM values are the ones which should be considered henceforth. Better fits were obtained with the inclusion of k_4 for runs with Mo^{3+} in excess, Figure 9. Runs in which $[H^+]$ was varied were also tested. Satisfactory fits were obtained with k_1, k_{-1}, k_2, and k_{-2} independent of $[H^+]$ (which we regard as established) but other solutions were possible, and the method was not sufficiently sensitive to enable a further refinement of data.

Discussion

The observation of three kinetic stages in the reaction of Mo^{3+} with O_2, along with the finding that ^{18}O is incorporated into the μ-oxo-bridging positions of the $Mo_2O_4^{2+}$ product, supports a reaction sequence (2)—(4). In this scheme a 1:1 adduct is first formed which proceeds *via* an intensely coloured dimeric intermediate through to $Mo_2O_4^{2+}$. Two inner-sphere reactions are involved, and bridging of the two Mo^{3+} ions by the O_2 is supported by ^{18}O incorporation into the $Mo_2O_4^{2+}$. Contributions from alternative reaction paths involving formation of Mo^{IV} and O_2^- in a single-electron outer-sphere process, or a two-electron change giving Mo^V and O_2^{2-}, are regarded as unlikely because of difficulties associated with the formation of monomeric Mo^{IV} and Mo^V. Furthermore, retention of the $Mo_2O_4^{2+}$ to O_2 stoicheiometry in equation (1) (1.03:1) does not suggest any significant contribution from these reactions. Moreover, the single-electron oxidant VO^{2+} (reduction potential 0.36 V) reacts only slowly with Mo^{3+}, rate constant 1×10^{-4} M^{-1} s^{-1},[17] and it would be surprising therefore if O_2 as a one-electron oxidant (−0.32 V for the O_2/HO_2 couple[27]) were to react with Mo^{3+} in an outer-sphere process at a rate constant of 180 M^{-1} s^{-1}. Neither is adduct formation in a 'dead-end' type mechanism with redox proceeding by an outer-sphere route supported by the above observations.

Kinetic studies (25 °C) on 1:1 substitution reactions of Mo^{3+} with NCS^- (rate constant 0.27 M^{-1} s^{-1}), Cl^- (0.0046 M^{-1} s^{-1}), and $HC_2O_4^-$ (0.49 M^{-1} s^{-1}) have been reported.[10,15] No dependence on $[H^+]^{-1}$ is observed and it has been concluded that the mechanism is I_a.[10,15] Rate constants obtained for the reaction of Mo^{3+} with O_2 (180 M^{-1} s^{-1}) and for MoO_2^{3+} with Mo^{3+} (40.5 M^{-1} s^{-1}) are also independent of $[H^+]$, and widen the range of values, consistent with an I_a process. Whether it is appropriate to consider a mechanism in which O_2 interacts at an octahedral face of the Mo^{3+} (d^3) ion with retention of a seven-co-ordinate product is not clear. Rapid processes which may have some of these features include the reaction of aliphatic radicals with V^{2+}.[28] Reactions of O_2 with ruthenium(II) complexes have now been shown to be outer-sphere.[2a]

The absence of an $[H^+]$ dependence for the 1:1 and 2:1 equilibration steps (2) and (3), $[H^+] = 1.0$—2.0 M, is highly relevant in considering possible structures for the two intermediates. In aqueous solution HO_2 is known to have a pK_a of 4.88,[29] and the pK_a of HO_2 bound to Co^{III} has been estimated as −1.[30] Taking due note of the latter an unprotonated bent co-ordinated superoxide is proposed for the 1:1 adduct. The second stage (3) can then understandably proceed without involvement of H^+ yielding the intensely coloured μ-peroxo-binuclear intermediate. If alternatively the 1:1 adduct is formally represented as Mo^V–O_2^{2-} with sideways bonding of the O_2^{2-} to the metal (a structure which is common for d^0 transition metals[31]), again the peroxide would not be expected to be protonated. Another possibility in view of the difficulty in generating monomeric Mo^{IV} is that the 1:1 adduct should be viewed as Mo^{3+}–O_2, with no significant transfer of charge. As yet, however, there are no established structures of this kind.

When O_2 is in excess no evidence for the MoO_2Mo^{6+} intermediate was obtained. In particular the first-order dependences on $[Mo^{3+}]$ and $[O_2]$ observed suggest that the intermediate MoO_2^{3+} does not proceed *via* MoO_2Mo^{6+} to the final product. Decomposition of MoO_2^{3+} to mononuclear Mo^V in the rate-determining step is presumably followed by rapid dimerisation to give the $Mo^V{}_2$ product. We note that k_4 is only an order of magnitude slower than k_3 for solutions 2.0 M in Hpts. For runs with Mo^{3+} in excess, KINSIM does give a better fit with the incorporation of k_4. Conversely, from the small variation of $k_{4(obs.)}$ with $[Mo^{3+}]$ (Table 3) it is possible that k_3 makes small contributions to $k_{4(obs.)}$. The full mechanism should therefore include reaction (10) alongside (2)—(4).

Acknowledgements

We are most grateful to Professor C. Frieden, for providing details of KINSIM, and to Professor J. H. Espenson for bringing this program to our attention. We wish to acknowledge an S.E.R.C. post-graduate studentship (to E. F. H.).

References

1 L. E. Bennett, *Prog. Inorg. Chem.*, 1973, **18**, 1; O. Hayaishi (ed.), 'Molecular Mechanisms of Oxygen Activation,' Academic Press, New York, 1974; F. Basolo, B. M. Hoffman, and J. A. Ibers, *Acc. Chem. Res.*, 1976, **9**, 175; T. G. Spiro (ed.), 'Metal Ion Activation of Dioxygen,' Wiley, New York, 1980; A. G. Sykes, *Adv. Inorg. Bioinorg. Mech.*, 1982, **1**, 121; J. F. Endicott and K. Kumar, *ACS Symp. Ser.*, 1982, **198**, 425; E. C. Niederhoffer, J. H. Timmons, and A. E. Martell, *Chem. Rev.*, 1984, **84**, 137.

2 (*a*) D. M. Stanbury, O. Hass, and H. Taube, *Inorg. Chem.*, 1980, **19**, 518; (*b*) I. I. Creaser, R. J. Geue, J. M. Harrowfield, A. J. Herlt, A. M. Sargeson, M. R. Snow, and J. Springborg, *J. Am. Chem. Soc.*, 1982, **104**, 6016; (*c*) A. Bakač, J. H. Espenson, I. I. Creaser, and A. M. Sargeson, *ibid.*, 1983, **105**, 7624.

3 S. Fallab and P. R. Mitchell, *Adv. Inorg. Bioinorg. Mech.*, 1984, **3**, 311.

4 A. G. Sykes and J. A. Weil, *Prog. Inorg. Chem.*, 1970, **13**, 1; R. G. Wilkins, *Adv. Chem. Ser.*, 1971, **100**, 111; G. McLendon and A. E. Martell, *Coord. Chem. Rev.*, 1976, **18**, 125.

5 R. M. Sellers and M. G. Simič, *J. Chem. Soc., Chem. Commun.*, 1975, 401; W. K. Wilmarth, H. Graff, and S. T. Gustin, *J. Am. Chem. Soc.*, 1956, **78**, 2683; M. Ardon and R. A. Plane, *ibid.*, 1959, **81**, 3197.

6 M. F. Tweedle and H. Taube, *Inorg. Chem.*, 1982, **21**, 3361.

7 P. George. *J. Chem. Soc.*, 1954, 4349; D-H. Chin, G. N. La Mar, and A. L. Balch, *J. Am. Chem. Soc.*, 1980, **112**, 4344.

8 J. S. Thompson, *J. Am. Chem. Soc.*, 1984, **106**, 4057; K. D. Karlin, Y. Gultneh, R. W. Cruse, J. C. Hayes, and J. Zubieta, *ibid.*, 3372.

9 L. K. Hanson and B. M. Hoffman, *J. Am. Chem. Soc.*, 1980, **102**, 4602.

10 Y. Sasaki and A. G. Sykes, *J. Chem. Soc., Chem. Commun.*, 1973, 767; *J. Chem. Soc., Dalton Trans.*, 1975, 1048.

11 Y. Sasaki and A. G. Sykes, *J. Chem. Soc., Dalton Trans.*, 1974, 1469.

12 M. Hahn and K. Wieghardt, *Inorg. Chem.*, 1984, **23**, 3977.

13 R. K. Murmann and M. E. Shelton, *J. Am. Chem. Soc.*, 1980, **102**, 3984.

14 D. T. Richens and A. G. Sykes, *Comm. Inorg. Chem.*, 1981, **1**, 141.

15 H. M. Kelly, D. T. Richens, and A. G. Sykes, *J. Chem. Soc., Dalton Trans.*, 1984, 1229.

16 D. T. Richens and A. G. Sykes, *Inorg. Synth.*, 1985, in the press.

17 D. T. Richens and A. G. Sykes, *J. Chem. Soc., Dalton Trans.*, 1984, 2099.

18 H. W. Stone and A. L. Eichelberger, *Anal. Chem.*, 1951, **23**, 868.

19 A. Seidell and W. F. Linke, 'Solubilities of Inorganic Compounds,' 4th edn., Van Nostrand, Princeton, N. J., 1964, p. 1228.

20 F. A. Cotton and S. H. Morehouse, *Inorg. Chem.*, 1965, **4**, 1380.

21 F. A. Armstrong, T. Shibahara, and A. G. Sykes, *Inorg. Chem.*, 1978, **17**, 189; W. S. McDonald, *Acta Crystallogr., Sect. B*, 1978, **34**, 2850.

22 M. A. Harmer, D. T. Richens, A. B. Soares, A. T. Thornton, and A. G. Sykes, *Inorg. Chem.*, 1981, **20**, 4155.

23 R. K. Murmann, *Inorg. Chem.*, 1980, **19**, 1765.

24 H. Gamsjäger and R. K. Murmann, *Adv. Inorg. Bioinorg. Mech.*, 1983, **2**, 317.

25 A. A. Frost and R. G. Pearson, 'Kinetics and Mechanism,' 2nd edn., Wiley, New York, 1961, p. 166.

26 B. A. Barshop, R. F. Wrenn, and C. Frieden, *Anal. Biochem.*, 1983, **130**, 134.

27 P. George, in 'Oxidases and Related Redox Systems,' University Park Press, Baltimore, Maryland, 1973, p. 1.

28 J-T. Chen and J. H. Espenson, *Inorg. Chem.*, 1983, **22**, 1651.

29 D. Behar, G. Czapski, J. Rakani, L. M. Dorman, and H. A. Schwarz, *J. Phys. Chem.*, 1970, **74**, 3209.

30 K. Kumar and J. F. Endicott, *Inorg. Chem.*, 1984, **23**, 2447.

31 See for example R. G. Thompson, *Inorg. Chem.*, 1984, **23**, 1794.

Received 4th March 1985; Paper 5/359